*Acta Cryst.* (1986). B42, 430-436

# Electron Density in Non-Ideal Metal Complexes. II. Sodium Bis(carbonato)cuprate(II)

BY E. N. MASLEN, N. SPADACCINI AND K. J. WATSON

*Crystallography Centre, University of Western Australia, Nedlands, Western Australia* 6009, *Australia*

AND A. H. WHITE

*Department of Physical and Inorganic Chemistry, University of Western Australia, Nedlands, Western Australia* 6009, *Australia*

(*Received* 7 *January* 1986; *accepted* 23 *May* 1986)

## Abstract

The room-temperature electron density distribution in crystals of $Na_2Cu(CO_3)_2$ has been determined from carefully measured and corrected X-ray diffraction data: $M_r = 229{\cdot}5$, monoclinic, $P2_1/a$, $a = 6{\cdot}170\ (2)$, $b = 8{\cdot}171\ (2)$, $c = 5{\cdot}648\ (2)$ Å, $\beta = 116{\cdot}24\ (1)°$, $V = 255{\cdot}4\ (1)$ Å$^3$, $Z = 2$, $D_x = 2{\cdot}985$ Mg mm$^{-3}$, Mo $K\alpha$, $\lambda = 0{\cdot}71069$ Å, $\mu = 4{\cdot}567$ mm$^{-1}$, $F(000) = 222$, $T = 298$ K, $R = 0{\cdot}026$ for 2696 reflections. Although the structural geometry of the $CuO_4$ moieties exhibits pseudo fourfold symmetry about the Cu atom, the corresponding difference density distribution does not. The deformation density near the Cu atom is such that regions of electron excess lie near the Na–Cu vectors, suggesting significant electron movement due to interactions with second-nearest-neighbour atoms. The magnitude of the density polarization by these second-nearest-neighbour interactions is of the same order as that by the nearest neighbours. The density near the Cu atom is also polarized by interactions with second-nearest-neighbour carbonate groups. This polarization has similar form to, but lower magnitude than, that due to the ligating carbonate oxygens.

## Introduction

The first paper in this series (Varghese & Maslen, 1985) directs attention to polarization of the electron density near the metal atoms in crystals of transition-metal complexes. The topological features in deformation density maps obtained using X-ray diffraction data indicate that part of this polarization is due to weaker forces in the crystal field. The nature of the second-nearest-neighbour interactions was not completely clarified, but similar effects occur in difference maps for a number of transition-metal complexes with non-ideal geometry. For example, Tanaka, Konishi & Marumo (1979) studied the charge density near the Cu atom in $KCuF_3$. Although qualitatively consistent with the redistribution of density predicted by the Jahn–Teller (1937) theorem, the idealized picture is modified in the crystal. Anisotropic features close to the copper nucleus have been ascribed to anharmonic thermal motion by Tanaka & Marumo (1982). Although this interpretation cannot be rejected until an accurate neutron diffraction analysis or low-temperature X-ray diffraction study has been made, the relationship of these features to the structure suggests that some of them arise from crystal-field interactions.

The electron density in crystals of potassium bis(carbonato)cuprate(II), $K_2Cu(CO_3)_2$ (Figgis, Reynolds, White & Williams, 1981), in which Cu shows approximately square-planar coordination, contains features near the Cu atom which do not have fourfold symmetry. These can be related to long-range interactions involving the Cu and K atoms and the carbonate groups (Maslen, Spadaccini & Watson, 1983). This structure is non-centrosymmetric, so the reliability of the difference density is limited. The crystal structure of the corresponding sodium salt, determined by Healy & White (1972), is centrosymmetric with low atomic thermal vibrations at room temperature. It is therefore well suited for a charge density study, to pursue in greater detail the effects of interactions with second-nearest neighbours.

## Experimental

Crystals of the anhydrous form of $Na_2Cu(CO_3)_2$ were prepared as described by Healy & White (1972). They are generally small pinacoids with average dimension approximately 0·1 mm, slightly elongated along **c**, but somewhat irregular in shape.

X-ray diffraction experiments with a number of crystals proved unsatisfactory since there were significant differences in the $\omega$–$2\theta$ scan profiles of measured intensities. This was demonstrated by disagreement between the integrated intensities of Friedel-pair-related reflections. The discrepancies were attributed to curvature in the crystals. A satisfactory crystal was eventually obtained and X-ray diffraction data suitable for a charge density study were measured at room temperature. Experimental details are given in Table 1. The irregularity in crystal shape necessitated an empirical absorption correction

0108-7681/86/050430-07$01.50 

(Flack, 1977). To account adequately for bias due to weak and negative net intensities, posterior estimates of the intensities were determined by a Bayesian statistics treatment (French & Wilson, 1978), assuming that the true values followed the probability distribution given by Wilson (1949) statistics. The treatment leads to improved posterior estimates of each intensity and its associated e.s.d.; these can be significant for the weaker reflections. The resulting 2696 independent structure amplitudes were all considered as observations in this analysis.

A weighted full-matrix least-squares refinement (based on $F$) of all the variable position and anisotropic thermal parameters, a scale factor and an isotropic secondary extinction factor (Larson, 1970), resulted in the atomic coordinates listed in Table 2.† The weights $w = 1/\sigma^2(F)$ are optimal in view of the care taken in determining e.s.d.'s for the structure amplitudes. Free-atom form factors of Cromer & Mann (1968) and the anomalous dispersion corrections of Cromer & Liberman (1970) for Na, Cu, C and O were used. The final agreement factors are given in Table 1. The isotropic extinction parameter, $r^* = 5{\cdot}0\,(2) \times 10^{-3}$, was small. Interatomic distances and angles for the structure are listed in Table 3. Standard crystallographic calculations were performed on a Perkin Elmer 3240 computer using the *XTAL* system (Stewart & Hall, 1983).

Table 1. *Experimental and refinement data*

| | |
|---|---|
| Diffractometer | Syntex $P2_1$ |
| Monochromator | Graphite |
| Scan type | $\omega$–$2\theta$ |
| Scan speed (° s$^{-1}$) min. | 0·081 |
| max. | 0·488 |
| Number of scans | 1 |
| Scan width ($a + b \tan\theta$) (°) | 2·3; 0·7 |
| Max. $2\theta$ (°) | 100 |
| Max. variation in intensity of standards ±200, ±020, ±003 (%) | 4 |
| Number of reflections measured | 11 350 (full sphere) |
| Transmission range in absorption correction | 0·70–0·89 |
| Internal agreement $R(I_o)$ | 0·017 |
| Number of averaged independent observations ($0 \le h \le 13$, $0 \le k \le 17$, $-12 \le l \le 10$) | 2696 |
| Final $R$ | 0·026 |
| Final $wR$ | 0·026 |
| Weights used | $1/\sigma^2(F_o)$ |
| Isotropic extinction factor $r^*$ where $\lvert F_c^*\rvert = k\lvert F_c\rvert(1 + 2r^*\lvert F_c\rvert^2\delta)^{-1/4}$ | $5{\cdot}0(2) \times 10^{-3}$ |
| Final max. shift/e.s.d. | 0·018 |
| Max. value of difference density (e Å$^{-3}$) | 1·2 (see Fig. 5) |
| Min. value of difference density (e Å$^{-3}$) | −1·4 (see Fig. 1) |

Table 2. *Fractional atomic coordinates and equivalent isotropic temperature factors with e.s.d.'s in parentheses*

| | $x$ | $y$ | $z$ | $U_{eq}$* (Å$^2 \times 10^5$) |
|---|---|---|---|---|
| Cu | 0 | 0 | 0 | 987 |
| Na | 0·67160 (8) | 0·09405 (5) | 0·35690 (8) | 1930 |
| O(1) | 0·32537 (10) | −0·08168 (7) | 0·21023 (13) | 1512 |
| O(2) | 0·36936 (11) | −0·28169 (7) | −0·03111 (12) | 1410 |
| O(3) | 0·40360 (13) | −0·33579 (8) | 0·37097 (14) | 1827 |
| C | 0·36569 (12) | −0·23665 (8) | 0·18683 (14) | 1112 |

* $U_{eq} = \frac{1}{6}\pi^2 \sum_i \sum_j \beta_{ij} \mathbf{a}_i . \mathbf{a}_j$.

## Structure

The crystal structure of $Na_2Cu(CO_3)_2$ has been described previously (Healy & White, 1972). It has square-planar $CuO_4$ moieties linked by bridging carbonate groups to form infinite sheets perpendicular to **c**.

Each $CuO_4$ moiety is strictly planar since the crystallographic symmetry at the copper site is $\bar{1}$. It also exhibits near-perfect fourfold symmetry with the Cu–O(1) and Cu–O(2) vectors 1·9436 (8) and 1·9332 (7) Å respectively with angles between them of 89·13 (3) and 90·87 (3)°.

The bridging carbonate ligands are distorted from ideal trigonal planar symmetry towards trigonal pyramidal, with the C atom 0·007(1) Å above and the O atoms 0·002(1) Å below the least-squares plane.‡ The C–O(1) and C–O(2) distances are extended owing to the involvement of these O atoms in bonding to Cu. The O(1)–C–O(2) angle is correspondingly decreased to 117·1 (1)°. The free O(3) is predominantly double bonded to C [1·256(1) Å] and the angles it makes to O(1) and O(2) [121·0(1) and 121·9 (1)°] are close to ideal. Differences in the C–O(1) and C–O(2) bond lengths noted by Healy & White (1972) were less pronounced in this analysis. Since this analysis is more accurate it is questionable whether different amounts of $p_\pi$ orbitals are involved in the interactions. The planes of the two symmetry-related carbonate groups bridging the $CuO_4$ moieties through O(1) and O(2) respectively are at angles of 97·29 (3) and 100·44 (3)° to the $CuO_4$ plane. The Cu atom is 1·625 (1) Å from the former but only 0·383 (1) Å from the latter; *i.e.* there is a significant twisting of the carbonate group away from the Cu–O(1) vector.

The Na atoms are interleaved between the $CuO_4$ moieties within each sheet, but not between sheets. Thus, beyond the nearest neighbours, each Cu atom has eight close contacts with Na atoms, being surrounded by two Na atoms very nearly in the $CuO_4$ plane, four Na atoms from $CuO_4$ planes centred at (1, 0, 0) and (−1, 0, 0) and two Na atoms from the $CuO_4$ planes centred at ($\frac{1}{2}$, $-\frac{1}{2}$, 0) and ($-\frac{1}{2}$, $\frac{1}{2}$, 0). The corresponding Cu–Na contact distances are 3·7998 (13), 3·3736 (12) and 3·5172 (10), 3·7815 (9) Å. Beyond the nearest-neighbour bridging

† Lists of structure amplitudes, anisotropic thermal parameters and least-squares planes have been deposited with the British Library Lending Division as Supplementary Publication No. SUP 42971 (12 pp.). Copies may be obtained through The Executive Secretary, International Union of Crystallography, 5 Abbey Square, Chester CH1 2HU, England.

‡ The results of least-squares plane calculations have been deposited. See deposition footnote.

Table 3. *Interatomic distances* (Å) *and angles* (°) *with e.s.d.'s in parentheses*

| | | | |
|---|---|---|---|
| Cu–O(1) | 1·9436 (8) | Cu–Na$^{vi}$ | 3·3736 (12) |
| Cu–O(2$^{ii}$) | 1·9332 (7) | Cu–Na$^{iii}$ | 3·5172 (10) |
| C–O(1) | 1·3084 (9) | Cu–Na$^{v}$ | 3·7815 (9) |
| C–O(2) | 1·2945 (12) | Cu–Na | 3·7998 (13) |
| C–O(3) | 1·2559 (11) | Cu–C$^{vii}$ | 4·8005 (16) |
| Cu–C$^{ii}$ | 2·6840 (9) | Cu–C$^{iii}$ | 4·8807 (14) |
| Cu–C | 2·7997 (9) | Cu–C$^{viii}$ | 4·9250 (12) |
| O(1)–Cu–O(2$^{ii}$) | 89·13 (3) | O(1)–C–O(2) | 117·07 (7) |
| O(1)–Cu–O(2$^{ix}$) | 90·87 (3) | O(1)–C–O(3) | 120·98 (8) |
| | | O(2)–C–O(3) | 121·93 (7) |

Symmetry code: (i) $1+x, y, z$; (ii) $\frac{1}{2}-x, \frac{1}{2}+y, -z$; (iii) $1-x, -y, -z$; (iv) $\frac{1}{2}-x, \frac{1}{2}+y, -z$; (v) $-\frac{1}{2}+x, \frac{1}{2}-y, z$; (vi) $-1+x, y, -1+z$; (vii) $\frac{1}{2}-x, -\frac{1}{2}+y, 1-z$; (viii) $1-x, -y, 1-z$; (ix) $-\frac{1}{2}+x, -\frac{1}{2}-y, z$.

with C atoms at 2·6840 (9) and 2·7997 (9) Å from Cu, there are three carbonate groups with C atoms at distances between 4·80 and 4·92 Å from Cu (Table 3).

## Electron density

The square-planar structure of the title compound is well suited to the study of longer-range interactions. Because the symmetry of the second-nearest neighbours is lower than that of the nearest neighbours, it is possible to differentiate between the two classes of interaction on the basis of the approximate symmetry of the difference maps. This contrasts with the situation in higher-symmetry structures such as diamond (Dawson, 1967; Price & Maslen, 1978) where the symmetries of the nearest and second-nearest neighbours produce effects which cannot be readily distinguished because the short- and long-range interactions have symmetry subgroups in common.

In structures where the environments of the atoms are complex, it is difficult to differentiate between different interactions. The limited number of interactions with second-nearest neighbours in the title compound allows their effects to be studied with less ambiguity. At large distances the charge on the carbonate group can be approximated by a point charge located at the carbon site. On this basis there are only seven crystallographically independent second-nearest-neighbour interactions (four to Na atoms and three to carbonate groups).

In charge density analysis of structures containing elements in the second and higher rows of the Periodic Table it is important to assess the amount of systematic error in the structure-factor data. Because of their high scattering power, uncorrected systematic error may have a marked effect on the deformation density near the heavier atoms. Study of the ratio $\Delta F/\sigma(F)$ *versus* $|F|$, $\sin\theta/\lambda$, $h, k$ and $l$ did not reveal any systematic trends. The change in density associated with the extinction correction is too small to account for the anisotropy in the density observed. There is no evidence for the presence of anisotropic extinction and we emphasize the excellent agreement between the intensities of equivalent reflections.

This anisotropy in density cannot be adequately modelled by anharmonic effects either. The density reaches a maximum and a minimum at distances of respectively 0·65 and 0·55 Å from the Cu nucleus. The high $\sin\theta/\lambda$ reflections, most affected by the anharmonic terms, do not exhibit any systematic discrepancies.

Becker, Coppens & Hirshfeld (1984) recommend the inclusion of $\sigma(\Delta\rho)$ as a guide to the size of random errors in the data. Because there is no theorem which entitles a feature in a continuous distribution to be declared 'not significant' on the basis of a point estimate of accuracy, we do not favour this recommendation. Notwithstanding our reservations, $\sigma(\Delta\rho)$ was evaluated using the formula given by Rees (1976). It is uniformly close to 0·07 e Å$^{-3}$ over most of the synthesis. Within 0·1 Å of the centre of the Cu atom $\sigma(\Delta\rho)$ increases, rising to its maximum value of 0·10 e Å$^{-3}$ at the nuclear position.

A preferable method for assessing the effects of random error on the deformation densities is to compare maps evaluated from different sets of structure factors. Maps were evaluated using the different sets of equivalent reflections with their values prior to averaging in the final data.

Three sections of the difference density in the vicinity of the Cu atom, evaluated with the averaged data, are given in Figs. 1(*a*), (*b*) and (*c*). Fig. 1(*a*) shows the plane containing the Cu, O(1) and O(2) atoms, Fig. 1(*b*) that including the Cu–O(1) bond and the normal to the O(1)–Cu–O(2) plane, and Fig. 1(*c*) the section through the Cu–O(2) bond and the normal to the O(1)–Cu–O(2) plane.

Figs. 2(*a*) and (*b*) are the same section as Fig. 1(*a*), evaluated with the independently measured structure factors, which give a guide to the random error in the deformation densities. The correspondence between the maps is closer than that observed in independent experiments from different laboratories (Coppens, 1984). Although the heights of the features in the maps vary by approximately one contour level, their shapes and locations are consistent, especially near the Cu atom.

In Fig. 1(*a*) the Cu atom is surrounded by an electron-deficient region (out to a radial distance of approximately 1 Å), with a diffuse annulus of lesser excess electron density between 1 and 2 Å. It is generally accepted that this represents 'promotion' of an electron from the inner $3d$ state to the outer more diffuse $4s$ state. The energy difference between the $3d^{10}4s^1$ and $3d^94s^2$ configurations is small enough for the perturbing potential due to the crystal field produced by the coordinated atoms to affect this promotion.

If nearest-neighbour interactions alone are considered it is difficult to account for all of the significant

difference-map features in Fig. 1. Whereas the Cu–O(1) and Cu–O(2) bonds are almost equal in length and perpendicular to one another, the difference density shows little indication of fourfold symmetry. The regions of electron deficiency along the Cu–O vectors may be interpreted qualitatively by considering nearest-neighbour interactions only. In the region of overlap the electron density is deficient because conflict between parallel spins requires reduction in density for fermions (Pauli, 1925). However, the magnitude of the deficiency along Cu–O(1) and Cu–O(2) differs significantly.

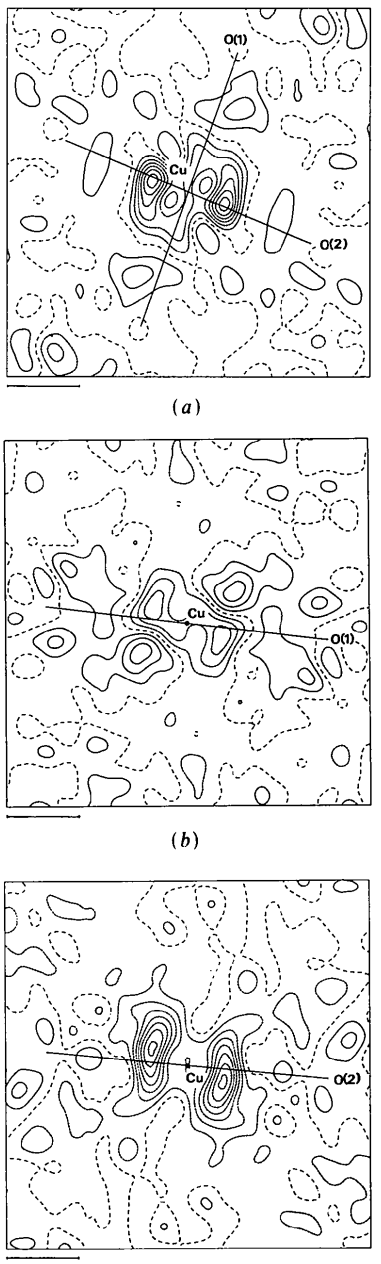


Fig. 1. Deformation density relative to independent spherical neutral atoms in sections containing (*a*) Cu, O(1) and O(2), (*b*) the Cu–O(1) bond and perpendicular to (*a*), (*c*) the Cu–O(2) bond and perpendicular to (*a*). The contour interval is 0·2 e Å$^{-3}$. Electron excess full lines; electron deficiency short dashes; zero contour dashed lines. The scale represents 1 Å.

In Fig. 1(*a*) there are two pairs of clearly resolved local maxima within 0·6 Å of the Cu nucleus. Lines joining the pairs are at right angles to each other and almost bisect the O(1)–Cu–O(2) angles. However, the distances from the Cu nucleus to the peaks not related by the centre of symmetry are different. Further, these peaks do not resemble one another even qualitatively in appearance. This suggests that other phenomena have a significant effect on the deformation density. A careful examination of the data, structure and density was made to identify the factors responsible for the lack of fourfold symmetry of Fig. 1(*a*). This asymmetry does not have any obvious relationship to crystal shape or to the geometry of the structure within the first coordination sphere. However, the long axis of the features along the diagonals lies close to short Cu–Na vectors in the structure.

The electron-deficient regions near the Cu atom are broadly similar to those observed in other Cu[II] complexes that have been studied. In this structure,

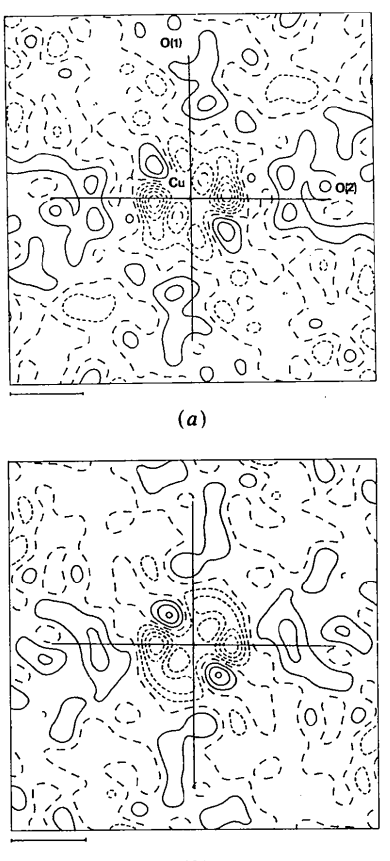


Fig. 2. Deformation density relative to independent spherical neutral atoms for the same section as Fig. 1(*a*) using two different data sets prior to averaging. Contours and scale as in Fig. 1.

these regions are both elongated perpendicular to and twisted away from the Cu–O vectors. In the plane of Fig. 1(*a*) the free carbonate oxygen O(3) lies 0·336(1) Å from the $CuO_4$ plane and makes an angle at Cu of about 40° to the Cu–O(1) vector. The O atom will be somewhat negatively charged and this leads to the extension of the deficient region in its direction. In the plane of Fig. 1(*c*) the same phenomenon occurs with the second-nearest-neighbour carbonate group. The Cu-C contact distance is 4·800 (2) Å and the region of electron deficiency extends in the direction of this group. Whereas there is significant electron deficiency near the Cu atom along the Cu–O vectors, this is not the case in the broader regions along the Cu-C contact directions.

Small features with excess residual density near the O atoms, lying almost directly on the Cu–O(1) and Cu-O(2) vectors (Fig. 1*a*), probably correspond to the oxygen lone pairs.

Fig. 3 is a section in the same plane as that of Fig. 1(*a*) but extending more than 5 Å from the Cu atom. The regions of electron excess 0·6 Å from the Cu nucleus lie close to the line of an Na-Cu [3·800 (1) Å] interaction. For the Na atom there is a broad maximum in the electron density approximately 0·4 Å from the nucleus. Density near the Na atom is slowly varying as a function of angle, as might be expected for a density function with a low rotational quantum number, *e.g.* an *s*-state atom. Similar characteristics were seen in an extended section of the plane in Fig. 1(*b*) which contains the Cu atom and four Na atoms. That the maxima do not lie exactly on the Na-Cu vector is probably due to the perturbing effect of other interactions such as those with the carbonate group. These were seen to be significant in determining the electron distribution in the potassium analogue of this compound (Figgis *et al.*, 1981). The Na-Cu interaction could be regarded as an incipient metal-metal bond, and it is interesting to note the similarity of the features observed here and those in stronger metal-metal bonds studied by Wang & Coppens (1976) and Mitschler, Rees & Lehmann (1978).

The effect of longer-range interactions is best illustrated in Figs. 4 and 5. The section in Fig. 4 passes exactly through two Cu and two Na atoms. This plane is shown in Fig. 6 as that containing Cu, $Cu^{i}$ and Na, $Na^{iii}$. The Cu-$Cu^{i}$ contact distance is 6·170 (2) Å, while the other contact distances, Cu-$Na^{iii}$ and Cu-Na, are 3·517 (1) and 3·800 (1) Å, respectively. The arrangement can thus be considered as three cations (one Cu and two Na) interacting with a Cu atom. Each interaction individually would generate electron excesses along the interaction vector. The total interaction is obviously cumulative (Hermansson, 1985); the relative displacement of the cations around the Cu atom should, therefore, lead to a strong electron excess directed along the Cu-Cu vector. Such a feature is indeed observed (Fig. 4). It cannot be related to the nearest-neighbour geometry and is clearly related to the second-nearest neighbours. A less striking but perhaps significant effect is the elongation of the electron-deficient regions near Cu toward the carbonate ions.

Fig. 5 shows the deformation density in a least-squares plane with two Cu atoms [displaced

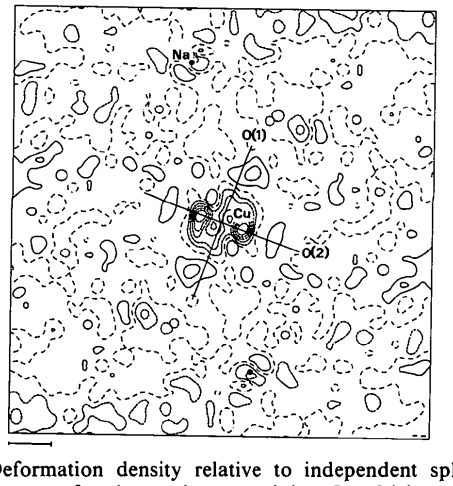


Fig. 3. Deformation density relative to independent spherical neutral atoms for the section containing Cu, O(1) and O(2) extending 5 Å from the Cu atom. Contours and scale as in Fig. 1.

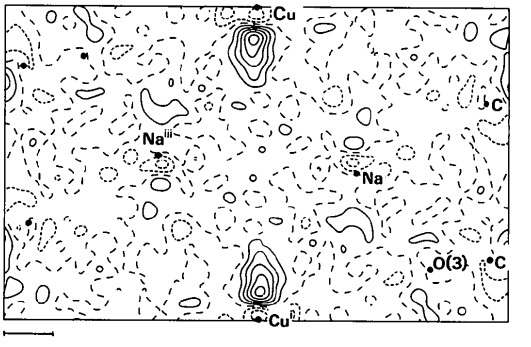


Fig. 4. Deformation density relative to independent spherical neutral atoms for the plane shown in Fig. 6 containing Cu, $Cu^{i}$ and Na, $Na^{iii}$. Contours and scale as in Fig. 1.

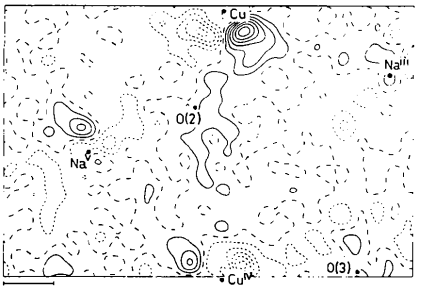


Fig. 5. Deformation density relative to independent spherical neutral atoms for the plane shown in Fig. 6 containing Cu, $Cu^{iv}$ and $Na^{iii,v}$. Contours and scale as in Fig. 1.

−0·166(1) and −0·110 (1) Å] and two Na atoms [displaced 0·121(1) and 0·155 (1) Å] almost in the plane. The plane is shown in Fig. 6 as that containing Cu, $Cu^{iv}$ and $Na^{iii,v}$. The Cu–Cu contact distance is 5·119 (1) Å while Cu–$Na^{v}$ is 3·7815 (9) Å. Unlike Fig. 4 this section contains an electronegative atom [O(2)] near the Cu–Cu vector. Cumulative interactions between cations of the type observed in Fig. 4 would not be observed, since that of Cu with O(2) contributes strongly to the difference density. However, a significant Cu–Na interaction is observed. Residual density of approximately 0·6 e $Å^{-3}$ lies along the $Cu^{iv}$–$Na^{v}$ vector. The residual density along the Cu–$Na^{iii}$ vector is the same as that in Fig. 4 in a different orientation.

Note also that the region of strong electron deficiency near the Cu atom at the bottom of Fig. 5 is directed approximately towards the shortest Cu–O(3) interaction [2·765 (1) Å] in the structure. The region of strongest deficiency in Fig. 4 (which is substantially weaker than those near Cu in Fig. 5) is directed along the line of the second-shortest Cu–O(3) contact of 3·593 (1) Å. Thus O(3), although not obviously bonded, participates in two significant interactions with Cu.

The deformation density in the plane through the carbonate group is consistent with other studies (Dunitz & Seiler, 1983). There is a modest amount of residual density (0·2 e $Å^{-3}$) along the C–O(1) and C–O(3) bonds, and 0·4 e $Å^{-3}$ in the C–O(2) bond.

## Conclusions

In structures of transition-metal complexes with geometry of near-to-ideal symmetry, such as $\gamma$-$Ni_2SiO_4$ (Marumo, Isobe, Saito, Yagi & Akimoto, 1974), it has been possible to explain the residual density near the transition-metal atoms in terms of models based on nearest-neighbour interactions alone. In the present case second-nearest-neighbour interactions must also be considered. The difference arises essentially because of the different symmetry of the second-nearest-neighbour environments in $Na_2Cu(CO_3)_2$. Similar effects for second-nearest neighbours may also occur in the case of deformation densities which have been previously explained in terms of nearest neighbours alone. They have not been identified in the deformation density because the identification was not assisted by differences in symmetry.

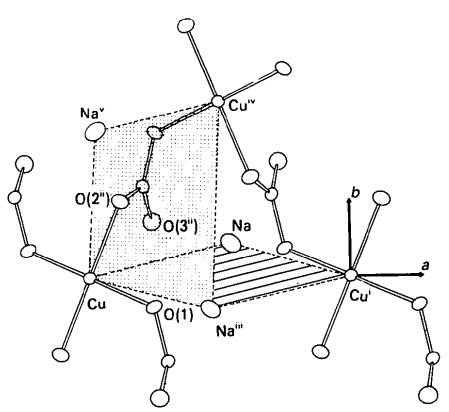


Fig. 6. Projection of the structure onto the *ab* plane. The planes of sections shown in Figs. 4 and 5 are highlighted. Superscripts are as in Table 3.

The relationship between the heights of the features along the interaction vectors is roughly comparable with the energies involved. The reduction in the classical electrostatic energy for the interacting free Cu and O atoms spaced 1·94 Å (the Cu–O bond distance) apart is −1·77 eV. That energy decreases rapidly with increasing Cu–O distance. The classical electrostatic energy for interacting Cu and Na atoms spaced 3·37 Å (the shortest Cu–Na distance) is −0·37 eV, which decreases more slowly with Cu–Na separation. This suggests that the significance of these second-nearest-neighbour interactions may be associated with the slow radial dependence of the electron density for the alkali-metal cations.

Recognition of the importance of some second-nearest-neighbour interactions on the difference density in crystalline solids may have important consequences. Theoretical calculations of difference densities for structures containing transition-metal atoms based on the assumption that nearest neighbours dominate the interactions will be inadequate in some cases. In structures with heavier atoms beyond the first transition series, interactions beyond the first coordination sphere may be even more significant.

The size of the deformation terms associated with the longer-range interactions also has implications for certain classes of spectroscopic experiment, which are often interpreted in terms of idealized models based on nearest-neighbour geometry. Conclusions based on such models may require modification if the effect of long-range interactions on the properties measured by the spectroscopic experiment is comparable with their effect on the deformation density. The orientation of the *g* tensor measured in the electron spin resonance (ESR) experiment may be significantly affected by longer-range interactions. Evidence for such an effect has been reported by Varghese & Maslen (1985) in the interpretation of the ESR results for copper sulfate pentahydrate.

Finally, the significance of second-nearest-neighbour interactions has implications for charge density analysis carried out either in direct space, based on the interpretation of deformation density maps, as in this case, or in reciprocal space, using such techniques as multipole refinements. In cases where the effects of second-nearest-neighbour interactions are significant the determination of population coefficients

for a limited set of multipole terms selected on the basis of the symmetry characteristics of the nearest-neighbour geometry alone will not be justified. In the structure described here, for example, the radial dependence in the regions of excess and deficient density near the Cu atom differ markedly. An efficient multipole representation of the density in terms of a limited set of angular and radial functions, based on the usual assumption that the electron density near each nucleus may be described as a separable sum of products of radial and angular functions, would almost certainly not be possible either in this or in other analogous cases. Theoretical studies are needed to complement this work, if only to confirm the magnitude of the effects involved.

Financial support for this project was provided by the Australian Research Grants Scheme and by the Research Committee of the University of Western Australia. One of us (NS) acknowledges receipt of a Commonwealth Postgraduate Award.

### References

BECKER, P. J., COPPENS, P. & HIRSHFELD, F. L. (1984). *J. Appl. Cryst.* **17**, 369.
COPPENS, P. (1984). *Acta Cryst.* A**40**, 184-195.
CROMER, D. T. & LIBERMAN, D. (1970). *J. Chem. Phys.* **53**, 1891-1898.
CROMER, D. T. & MANN, J. B. (1968). *Acta Cryst.* A**24**, 321-324.
DAWSON, B. (1967). *Proc. R. Soc. London Ser. A*, **298**, 264-288.
DUNITZ, J. D. & SEILER, P. (1983). *J. Am. Chem. Soc.* **105**, 7056-7058.
FIGGIS, B. N., REYNOLDS, P. A., WHITE, A. H. & WILLIAMS, G. A. (1981). *J. Chem. Soc. Dalton Trans.* pp. 371-376.
FLACK, H. D. (1977). *Acta Cryst.* A**33**, 890-898.
FRENCH, S. & WILSON, K. (1978). *Acta Cryst.* A**34**, 517-525.
HEALY, P. C. & WHITE, A. H. (1972). *J. Chem. Soc. Dalton Trans.* pp. 1913-1917.
HERMANSSON, K. (1985). *Acta Cryst.* B**41**, 161-169.
JAHN, H. A. & TELLER, E. (1937). *Proc. R. Soc. London Ser. A*, **161**, 220-235.
LARSON, A. C. (1970). *Crystallographic Computing*, edited by F. R. AHMED. Copenhagen: Munksgaard.
MARUMO, F., ISOBE, M., SAITO, Y., YAGI, T. & AKIMOTO, S. (1974). *Acta Cryst.* B**30**, 1904-1906.
MASLEN, E. N., SPADACCINI, N. & WATSON, K. J. (1983). *Proc. Indian Acad. Sci.* **92**, 443-448.
MITSCHLER, A., REES, B. & LEHMANN, M. S. (1978). *J. Am. Chem. Soc.* **100**, 3390-3397.
PAULI, W. (1925). *Z. Phys.* **31**, 765.
PRICE, P. F. & MASLEN, E. N. (1978). *Acta Cryst.* A**34**, 173-183.
REES, B. (1976). *Acta Cryst.* A**32**, 483-488.
STEWART, J. M. & HALL, S. R. (1983). *The XTAL System of Crystallographic Programs.* Tech. Rep. TR-1364.1. Computer Science Center, Univ. of Maryland, College Park, Maryland.
TANAKA, K., KONISHI, M. & MARUMO, F. (1979). *Acta Cryst.* B**35**, 1303-1308.
TANAKA, K. & MARUMO, F. (1982). *Acta Cryst.* B**38**, 1422-1427.
VARGHESE, J. N. & MASLEN, E. N. (1985). *Acta Cryst.* B**41**, 184-190.
WANG, Y. & COPPENS, P. (1976). *Inorg. Chem.* **15**, 1122-1127.
WILSON, A. J. C. (1949). *Acta Cryst.* **2**, 318-321.

*Acta Cryst.* (1986). B**42**, 436-442

# X-ray Diffraction Study of Short-Range-Ordered Structure in a Disordered Ag–15·0 at.% Mg Alloy

BY KEN-ICHI OHSHIMA* AND JIMPEI HARADA

*Department of Applied Physics, Nagoya University, Nagoya* 464, *Japan*

(*Received* 24 *January* 1986; *accepted* 25 *March* 1986)

### Abstract

Short-range-order (SRO) parameters of disordered Ag–15·0 at.% Mg alloy were determined at room temperature from an analysis of the X-ray diffuse scattering by applying the Borie & Sparks [*Acta Cryst.* (1971), A**27**, 198-201] separation method. The SRO parameters beyond the 20th-neighbor shell were found to play an important role in characterizing a fourfold splitting of the diffuse scattering. Computer-simulated local Mg-atom arrangement in a f.c.c. lattice showed the existence of $Cu_3Au$-type ordered regions of one or two unit-cell dimensions connected with antiphase relations. Comparison of the atomic-pair interaction potential obtained from the SRO diffuse scattering and the form of the long-range interaction attributed to conduction-electron screening of the ions led to the deduction that the Fermi surface of this alloy has some resemblance to that of a noble metal.

## 1. Introduction

Characteristic fourfold splittings of diffuse scattering have been observed at the 100, 110 and equivalent positions on the electron and X-ray diffraction patterns from disordered or quenched states of several binary alloys with a face-centered cubic structure [Cu-Au: Raether (1954); Sato, Watanabe & Ogawa

* Present address: Institute of Applied Physics, University of Tsukuba, Sakura, Ibaraki 305, Japan.

0108-7681/86/050436-07$01.50 